Using graded barriers to control the optical properties of ZnO/$Zn_{0.7}Mg_{0.3}O$ quantum wells with an intrinsic internal electric field

C. R. Hall,[1] L. V. Dao,[1] K. Koike,[2] S. Sasa,[2] H. H. Tan,[3] M. Inoue,[2] M. Yano,[2] C. Jagadish,[3] and J. A. Davis[1,a)]

[1]*Centre for Atom Optics and Ultrafast Spectroscopy, Swinburne University of Technology, Melbourne 3122, Australia*

[2]*Nanomaterials Microdevices Research Centre, Osaka Institute of Technology, Asahi-ku Ohmiya, Osaka 535-8585, Japan*

[3]*Department of Electronic Materials Engineering, Research School of Physics and Engineering, The Australian National University, Canberra, Australian Capital Territory 0200, Australia*

(Received 30 March 2010; accepted 16 April 2010; published online 14 May 2010)

Quantum wells with graded barriers are demonstrated as a means to control both the transition energy and electron-hole wave function overlap for quantum wells with an intrinsic internal electric field. In the case of *c*-axis grown ZnO/ZnMgO quantum wells, the graded barriers are produced by stepping the magnesium composition during the growth process. Four quantum wells with different structures are examined, where each well has similar transition energy, yet a wide range of wave function overlaps are observed. Photoluminescence and time resolved photoluminescence show good agreement with calculations. © *2010 American Institute of Physics*. [doi:10.1063/1.3428430]

ZnO is a wide band-gap semiconductor which has recently received much attention due to its potential for application in devices that are optically active in the ultraviolet spectral region.[1–4] Driving this interest in ZnO are the large exciton and biexciton binding energies (60 meV and 15 meV, respectively), low growth temperatures and low material cost, offering several advantages over GaN, the predominant material for such device applications.[3,5,6]

The development of high quality ZnO thin film growth[7,8] techniques has allowed the growth of ZnO/ZnMgO quantum wells (QWs),[9] and studies of their properties as a function of well width,[10–13] barrier height,[10,14] and excitation intensity[11,15] have followed. Characterization of QW structures forms the basis for the development of QW based devices such as lasers, selective energy photodiodes,[16] and light emitting diodes. These devices take advantage of quantum confinement effects, providing the ability to tune the transition energy[17] and an enhancement of the exciton binding energy.[18]

In wurtzite, *c*-axis grown ZnO/ZnMgO QWs, the mismatch of spontaneous polarizations at the well-barrier interfaces results in an intrinsic electric field across the QW.[11] A piezoelectric polarization also exists in this II-VI system, however, this is in the opposite direction to, and is weaker than the spontaneous polarization at the ZnO/ZnMgO interface.[15,19] The resulting built-in electric field redshifts the transition energy, even below the band gap of bulk ZnO in sufficiently wide wells.[13] The electrons and holes become spatially separated, consequently reducing the oscillator strength and increasing the radiative lifetime of the dominant E1-H1 transition.[13,20,21] The exciton binding energy is also reduced by the electric field, counteracting any enhancement normally associated with quantum confinement.[11] For a comprehensive discussion of the dynamics of the quantum confined Stark effect (QCSE) in square ZnO QWs see Ref. 21.

It is known that the combination of structured QWs and an externally applied electric field may be used as an additional means of control over the optical properties of QWs.[22,23] Structured QWs have recently been demonstrated as a possible method for countering an intrinsic QCSE in GaN based QWs.[24,25] Recently, intermixing induced by ion implantation and rapid thermal annealing was demonstrated as a means to control the band profile and hence the optical properties of ZnO QWs with an intrinsic QCSE.[13,26] Increases in both the QW transition energy and E1-H1 wave function overlap were observed. Ion implantation as a means to produce QWs with graded barriers is, however, limited.[13]

In this letter, we show that as-grown graded barrier QWs in conjunction with an intrinsic QCSE can be used to "tune" the E1-H1 wave function overlap (and thus oscillator strength), while overcoming the issues of ion implantation induced intermixing.

Our single QW samples were grown by plasma-assisted molecular beam epitaxy (MBE) on *a*-plane Al_2O_3 substrates, and consist of a 15 nm low temperature $Zn_{0.9}Mg_{0.1}O$ buffer layer followed by a 400 nm $Zn_{0.7}Mg_{0.3}O$ layer which also forms the barrier on one side of the QW. The subsequent growth of the QW was followed by a 50 nm $Zn_{0.7}Mg_{0.3}O$ barrier layer which doubled as the capping layer. All the layers were nominally undoped. The surface and bottom ZnMgO barrier layers were grown at 350 °C to avoid the phase separation into wurtzite ZnO-rich and rocksalt MgO-rich domains although the ZnO well layer was grown at 500 °C. The growth profiles for the graded barrier structures we examined are shown in Fig. 1, which shows a step size of 1 nm, or approximately two ZnO unit cells, where the lattice constant along the *c*-axis is 5.2 Å.[3] During the graded barrier growth, a growth-interruption of 2 min was introduced at respective heterointerfaces to make the interface abrupt, and the Mg composition of respective layers was controlled by changing Mg flux under a Zn-excess condition with constant O_2 and Zn fluxes. Detail of the composition control has been described elsewhere.[1,27] In this letter, the graded barrier QWs

a)Electronic mail: jdavis@swin.edu.au.

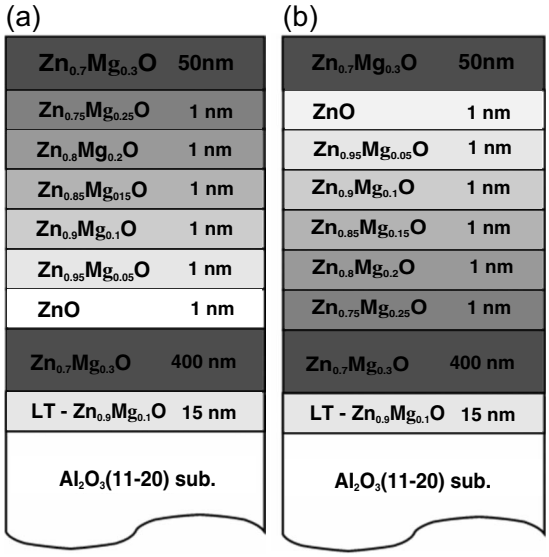

FIG. 1. Growth profile of the two graded barrier samples. (a) Sample S1. (b) Sample S2.

are compared to 2 and 4 nm square QWs. Each layer for the graded and square QWs was *c*-axis oriented single-crystal with O-polar surface. In the case of a square well with 30% Mg composition in the barrier and 0% in the well, an internal electric field of 900 kV/cm is expected.[13]

Sample S1 (sample S2) is grown so that the valance band (conduction band) steps in the opposite direction to the internal electric field which "flattens out" the band profile. The resulting potential profiles, together with calculated electron and hole wave functions (calculated assuming a one-dimensional potential based on these profiles), are shown in Fig. 2. The calculations used a conduction band/valence band offset of 70/30, a ZnO ($Zn_{0.7}Mg_{0.3}O$) band gap at 20 K of 3.43 eV (4.12 eV), and electron (hole) effective mass of 0.28 (0.78).

Based on these calculations, the E1-H1 wave function overlaps are 0.25 and 0.71, and the transition energies 3.52 eV and 3.57 eV for samples S1 and S2, respectively. In the absence of any internal electric field, both of these values would be identical in the two samples. The presence of the electric field, combined with the 70:30 band offset ratio, causes them to differ substantially. Consider, for example, the valence band in S1 and conduction band in S2; were the offset ratio 50:50, these would be mirror images of each

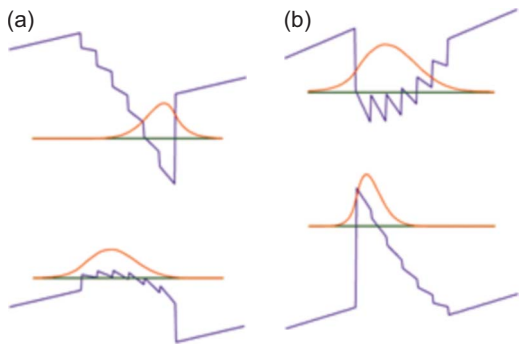

FIG. 2. (Color online) The potential profiles and calculated wave function amplitudes for samples S1 and S2 including the effects of the internal electric field. This is evident in the overlap integrals of 0.25 and 0.71 for samples S1 and S2, respectively.

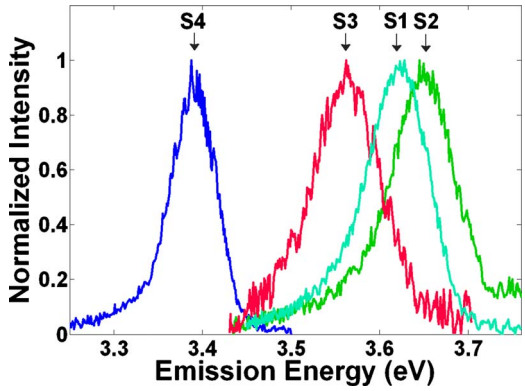

FIG. 3. (Color online) PL spectra for S1, S2, S3, and S4 at 20 K.

other. In reality however, the height of the potential steps in the two samples are not the same, which combined with an E-field that remains unchanged, leads to potential profiles for S1 and S2 which are not simply mirror images of each other. The effect of this can be seen in Fig. 2, where the valence band of S1 is substantially flatter than the conduction band in S2. A similar argument may be made for the different effective band profiles for the conduction (valence) band of sample S1 (S2) and explains the expected differences in wave function overlap and transition energy.

Photoluminescence (PL) spectra were recorded using a scanning monochromator equipped with a photomultiplier tube. The samples were optically excited by 100 fs pulses at a repetition rate of 80 MHz with photon energy 4.66 eV and an excitation density of 4.5 μJ cm^{-2} per pulse. Time resolved PL (TRPL) with 20 ps time resolution was obtained using a streak camera coupled to an imaging spectrometer. For all measurements the samples were maintained at a temperature of 20 K.

The PL spectrum for each sample is shown in Fig. 3. The measured and calculated transition energies and wave function overlaps are presented in Table I for comparison. Each of the samples show emission slightly higher than the calculated values, these, however, do not include exciton binding energy, which will be different in each sample and different to the bulk ZnO value due to quantum confinement effects. The implication is that the calculated transition energies will be further redshifted when the exciton binding energy is included and will therefore be even lower than the measured values. These discrepancies may suggest that the wells are slightly narrower than intended and for samples S1 and S2, there may also be a blueshift caused by a lower than anticipated internal electric field due to a greater strain induced piezoelectric field resulting from the multiple interfaces. The

TABLE I. Calculated transition energies and wave function overlaps, compared to experimental values for the lifetimes, measured by TRPL and transition energies. The calculated transition energies do not include exciton binding energy.

Sample	Measured t_c (ps)	Measured E (eV)	Calculated overlap	Calculated E (eV)
S1	1791 (±50)	3.56 (±0.01)	0.25	3.52
S2	847 (±12)	3.62 (±0.01)	0.71	3.57
S3	781 (±10)	3.65 (±0.01)	0.86	3.58
S4	1041 (±13)	3.39 (±0.01)	0.36	3.38

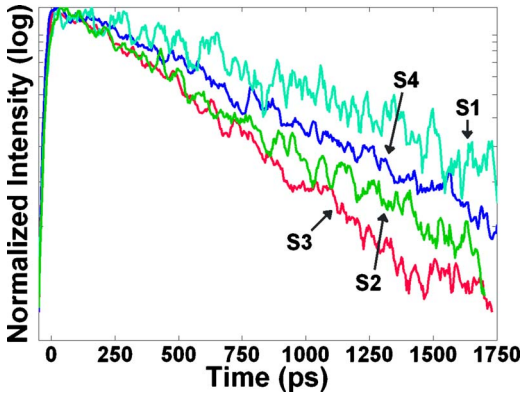

FIG. 4. (Color online) TRPL for samples S1, S2, S3, and S4 at 20 K. The shorter recombination lifetime for sample S2 when compared to sample S1 suggests that the E1-H1 wave function overlap for sample S2 is greater than that in sample S1.

calculated transition energies do, however, follow the same trend as the measured values, suggesting a small systematic error.

TRPL is used to examine the electron-hole wave function overlap based on the following relation:

$$T_1 \propto \frac{1}{|\langle \psi_e | \psi_h \rangle|^2}, \tag{1}$$

where the radiative lifetime (T_1) is proportional to the inverse of the square of the wave function overlap. Equation (1), however, does not consider other recombination processes which may not follow this relation. The recorded TRPL are shown in Fig. 4. The recombination lifetime for S2 (847 ps) is shorter than that of S1 (1791 ps), suggesting that the E1-H1 wave function overlap in S2 is greater than in S1, in agreement with the calculated overlaps (0.71 and 0.25, respectively). Measured decay times for samples S4 (1041 ps) and S3 (781 ps) also follow the trend predicted by the calculated electron-hole wave function overlaps (0.36 and 0.86). The measured lifetimes and calculated wave function overlaps are shown in Table I, and while they follow the right trend across all four samples, they do not fit Eq. (1) exactly. The possibility that carrier induced shielding is responsible for these discrepancies is ruled out as in each case the data were well fit by a single exponential decay, rather than a continuously varying decay as reported previously.[21] The failure of the measured TRPL to follow Eq. (1) exactly is probably due to the presence of non-radiative processes, possibly associated with defects and/or carrier/phonon scattering, and which appear to be present in all cases.

In conclusion, we have demonstrated that graded barrier QWs can be used to control the optical properties of QWs with an intrinsic internal electric field. For a series of samples with different barrier designs we calculated E1-H1 wave function overlap integrals and measured the corresponding lifetimes. The calculated overlaps varied from 0.86 to 0.25 and the corresponding measured lifetimes varied from 781 ps to 1.7 ns, increasing with decreasing overlap as expected. This ability to predictably control the wave function overlap and transition energy using graded barriers in QWs under the influence of the QCSE adds to the commonly used techniques for tuning QW properties, including well width, band gap, and barrier height.

Australian Research Council is gratefully acknowledged for financial support. C.R.H. thanks Lastek for financial support.

[1]C. Jagadish and S. J. Pearton, *Zinc Oxide Bulk, Thin Films and Nanostructures* (Elsevier, Oxford, 2006).
[2]A. Janotti and C. G. Van De Walle, Rep. Prog. Phys. **72**, 126501 (2009).
[3]Ü. Özgür, Y. I. Alivov, C. Liu, A. Teke, M. A. Reshchikov, S. Dogan, V. Avrutin, S. J. Cho, and H. Morkoc, J. Appl. Phys. **98**, 041301 (2005).
[4]J. A. Davis and C. Jagadish, Laser Photonics Rev. **3**, 85 (2009).
[5]K. Okada, Y. Yamada, T. Taguchi, F. Sasaki, S. Kobayashi, T. Tani, S. Nakamura, and G. Shinomiya, Jpn. J. Appl. Phys., Part 2 **35**, L787 (1996).
[6]J. W. Orton and C. T. Foxon, Rep. Prog. Phys. **61**, 1 (1998).
[7]P. Zu, Z. K. Tang, G. K. L. Wong, M. Kawasaki, A. Ohtomo, H. Koinuma, and Y. Segawa, Solid State Commun. **103**, 459 (1997).
[8]Y. Chen and D. M. Bagnall, J. Appl. Phys. **84**, 3912 (1998).
[9]A. Ohtomo, M. Kawasaki, I. Ohkubo, H. Koinuma, T. Yasuda, and Y. Segawa, Appl. Phys. Lett. **75**, 980 (1999).
[10]T. Makino, C. H. Chia, N. T. Tuan, H. D. Sun, Y. Segawa, M. Kawasaki, A. Ohtomo, K. Tamura, and H. Koinuma, Appl. Phys. Lett. **77**, 975 (2000).
[11]C. Morhain, T. Bretagnon, P. Lefebvre, X. Tang, P. Valvin, T. Guillet, B. Gil, T. Taliercio, M. Teisseire-Doninelli, B. Vinter, and C. Deparis, Phys. Rev. B **72**, 241305(R) (2005).
[12]T. Guillet, T. Bretagnon, T. Taliercio, P. Lefebvre, B. Gil, C. Morhain, and X. Tang, Superlattices Microstruct. **41**, 352 (2007).
[13]J. A. Davis, L. V. Dao, X. Wen, C. Ticknor, P. Hannaford, V. A. Coleman, H. H. Tan, C. Jagadish, K. Koike, S. Sasa, M. Inoue, and M. Yano, Nanotechnology **19**, 055205 (2008).
[14]T. Bretagnon, P. Lefebvre, T. Guillet, T. Taliercio, B. Gil, and C. Morhain, Appl. Phys. Lett. **90**, 201912 (2007).
[15]M. Yano, K. Hashimoto, K. Fujimoto, K. Koike, S. Sasa, M. Inoue, Y. Uetsuji, T. Ohnishi, and K. Inaba, J. Cryst. Growth **301-302**, 353 (2007).
[16]T. H. Wood, C. A. Burrus, A. H. Gnauck, J. M. Wiesenfeld, D. A. B. Miller, D. S. Chemla, and T. C. Damen, Appl. Phys. Lett. **47**, 190 (1985).
[17]R. Dingle, W. Wiegmann, and C. H. Henry, Phys. Rev. Lett. **33**, 827 (1974).
[18]H. D. Sun, T. Makino, Y. Segawa, M. Kawasaki, A. Ohtomo, K. Tamura, and H. Koinuma, J. Appl. Phys. **91**, 1993 (2002).
[19]M. W. Allen, P. Miller, R. J. Reeves, and S. M. Durbin, Appl. Phys. Lett. **90**, 062104 (2007).
[20]D. A. B. Miller, D. S. Chemla, T. C. Damen, A. C. Gossard, W. Wiegmann, T. H. Wood, and C. A. Burrus, Phys. Rev. Lett. **53**, 2173 (1984).
[21]C. R. Hall, L. Dao, K. Koike, S. Sasa, H. H. Tan, M. Inoue, M. Yano, P. Hannaford, C. Jagadish, and J. A. Davis, Phys. Rev. B **80**, 235316 (2009).
[22]W. Chen and T. G. Andersson, Semicond. Sci. Technol. **7**, 828 (1992).
[23]J. Thalken, W. Li, S. Haas, and A. F. J. Levi, Appl. Phys. Lett. **85**, 121 (2004).
[24]L. Wang, R. Li, Z. Yang, D. Li, T. Yu, N. Liu, L. Liu, W. Chen, and X. Hu, Appl. Phys. Lett. **95**, 211104 (2009).
[25]H. P. Zhao, G. Y. Liu, X. H. Li, R. A. Arif, G. S. Huang, J. D. Poplawsky, S. Tafon Penn, V. Dierolf, and N. Tansu, IET Optoelectron. **3**, 283 (2009).
[26]V. A. Coleman, M. Buda, H. H. Tan, C. Jagadish, M. R. Phillips, K. Koike, S. Sasa, M. Inoue, and M. Yano, Semicond. Sci. Technol. **21**, L25 (2006).
[27]M. Yano, K. Ogata, F. P. Yan, K. Koike, S. Sasa, and M. Inoue, *Progress in Semiconductor Materials II - Electronic and Optoelectronic Applications*, edited by B. D. Weaver, M. O. Manasreh, C. Jagadish, and S. Zollner, MRS Symposia Proceedings No. 744 (Materials Research Society, Pittsburgh, 2003), p. M3.1.